Silica Nanostructures Templated by Oriented Block Copolymer Thin Films Using Pore-Filling and Selective-Mineralization Routes

Brian J. Melde and Sandra L. Burkett*

Department of Chemistry, Amherst College, Amherst, Massachusetts 01002

Ting Xu, James T. Goldbach, and Thomas P. Russell*

Department of Polymer Science and Engineering, University of Massachusetts, Amherst, Massachusetts 01003

Craig J. Hawker

Department of Chemistry and Biochemistry, University of California, Santa Barbara, California 93106

Received June 29, 2005

Poly(styrene-*block*-methyl methacrylate) thin films with cylindrical microdomains oriented normal to the surface were used as templates for nanoscopic silica structures. Silicon oxide was synthesized using vapor-phase and liquid-phase sol−gel reactions of tetraethoxysilane (TEOS). The vapor-phase reaction selectively formed silicon oxide within the poly(methyl methacrylate) (PMMA) domains. The use of liquid sols led to reconstruction of the film by selective solvation of the PMMA chains, followed by mineralization of silicon oxide. In addition, the vapor-phase and liquid-phase reactions were used to deposit silica in porous polystyrene (PS) films made by selective etching of the PMMA cylinders. Removal of polymer by calcination in air at 500 °C resulted in ordered arrays of silica nanostructures. Dynamic wettability measurements were made on nanostructured surfaces after functionalization with hydrophobic organosilanes.

Introduction

Silicon oxide is useful as a coating or substrate because of its transparency in the visible spectrum, its hardness, and its low dielectric constant. The presence of silanol (SiOH) groups allows silica surfaces to be functionalized for applications such as biosensing,[1−3] cell culture growth,[4] heterogeneous catalysis,[5] and wettability.[6,7] Numerous efforts have been made to control the nanometer-scale morphology of silica surfaces to enable applications. The hydrophobicity of a silica surface can be influenced significantly by surface topography as tailored by lithographic techniques;[7] ultralow dielectric constants, which are necessary for future microelectronics technology, have been achieved through the use of block copolymers or surfactants to template mesopores in silicate films.[8−12]

Block copolymers are effective and versatile templates for inorganic materials with ordered structures on the nanometer scale. They allow a smaller size scale of structure to be synthesized compared to conventional lithographic techniques; the size of a nanostructure can be controlled most directly by choice of copolymer molecular weight. Depending on volume fraction and segmental interactions, diblock copolymers can microphase separate into body-centered-cubic-packed spheres, hexagonally close-packed cylinders, a gyroid with cubic symmetry, or lamellae.

In solution, micellar assemblies[13,14] and liquid crystals[15,16] of block copolymers have been used to template various silica mesostructures. The difference in hydrophilicity between the blocks of the bulk copolymer has been exploited for controlled mineralization of metal oxides by sol−gel chem-

* To whom correspondence should be addressed. (S.L.B.): Phone: (413) 542−2730; fax: (413) 542−2735; e-mail: slburkett@amherst.edu. (T.P.R.): Phone: (413) 545-2680; fax: (413) 577-1510; e-mail: russell@mail.pse.umass.edu.

(1) Chee, M.; Yang, R.; Hubbell, E.; Berno, A.; Huang, X. C.; Stern, D.; Winkler, J.; Lockhart, D. J.; Morris, M. S.; Fodor, S. P. A. *Science* **1996**, *274*, 610.
(2) Fodor, S. P. A. *Science* **1997**, *277*, 393.
(3) Kambhampati, D. K.; Jakob, T. A. M.; Robertson, J. W.; Cai, M.; Pemberton, J. E.; Knoll, W. *Langmuir* **2001**, *17*, 1169.
(4) Rühe, J.; Yano, R.; Lee, J. S.; Köberle, P.; Knoll, W.; Offenhäusser, A. *J. Biomater. Sci., Polym. Ed.* **1999**, *1999*, 859.
(5) Petrucci, M. G. L.; Kakkar, A. K. *Chem. Mater.* **1999**, *11*, 269.
(6) Fadeev, A. Y.; McCarthy, T. J. *Langmuir* **1999**, *15*, 3759.
(7) Öner, D.; McCarthy, T. J. *Langmuir* **2000**, *16*, 7777.
(8) Lu, Y.; Fan, H.; Doke, N.; Loy, D. A.; Assink, R. A.; LaVan, D. A.; Brinker, C. J. *J. Am. Chem. Soc.* **2000**, *122*, 5258.
(9) Wirnsberger, G.; Yang, P.; Scott, B. J.; Chmelka, B. F.; Stucky, G. D. *Spectrochim. Acta A* **2001**, *57*, 2049.
(10) Yang, S.; Mirau, P. A.; Pai, C.-S.; Nalamasu, O.; Reichmanis, E.; Lin, E. K.; Lee, H.-J.; Gidley, D. W.; Sun, J. *Chem. Mater.* **2001**, *13*, 2762.
(11) Yang, S.; Mirau, P. A.; Pai, C.-S.; Nalamasu, O.; Reichmanis, E.; Pai, J. C.; Obeng, Y. S.; Seputro, J.; Lin, E. K.; Lee, H.-J.; Sun, J.; Gidley, D. W. *Chem. Mater.* **2002**, *14*, 369.
(12) Pai, R. A.; Humayun, R.; Schulberg, M. T.; Sengupta, A.; Sun, J.-N.; Watkins, J. J. *Science* **2004**, *303*, 507.
(13) Zhao, D.; Feng, J.; Huo, Q.; Melosh, N.; Fredrickson, G. H.; Chmelka, B. F.; Stucky, G. D. *Science* **1998**, *279*, 548.
(14) Zhao, D.; Huo, Q.; Feng, J.; Chmelka, B. F.; Stucky, G. D. *J. Am. Chem. Soc.* **1998**, *120*, 6024.
(15) Melosh, N. A.; Davidson, P.; Chmelka, B. F. *J. Am. Chem. Soc.* **2000**, *122*, 823.
(16) Feng, P.; Bu, X.; Stucky, G. D.; Pine, D. J. *J. Am. Chem. Soc.* **2000**, *122*, 994.

10.1021/cm051407b CCC: $30.25
Published on Web 08/13/2005

istry. Wiesner and co-workers have synthesized aluminum silicates in the PEO blocks of poly(isoprene-*block*-ethylene oxide) (P(I-*b*-EO))[17,18] and poly(ethylene oxide-*b*-*n*-hexyl methacrylate)[19,20] using aluminum *sec*-butoxide and 3-(glycidyloxypropyl)trimethoxysilane, which selectively swell the PEO blocks. Changing the amount of aluminum silicate precursors and altering the molecular weight of P(I-*b*-EO) influenced the morphologies and dimensions of the resulting nanocomposites. Selective swelling of the hydrophobic domains produced nanoscale objects of different sizes and shapes, and calcination of selected products resulted in mesoporous ceramics.

Lateral arrays of nanostructured silicon oxides that might have applications in on-chip and separation technologies have previously been created from films of self-assembled block copolymers. Nanoporous and nanorelief silicon oxycarbide ceramic films have been fabricated by oxidation of poly(isoprene-*b*-pentamethyldisilylstyrene-*b*-isoprene);[21] ozonolysis and UV radiation removed the hydrocarbon and formed ceramic from the silicon-containing block. Ordered arrays of nanoscopic silica posts have been etched into a silicon oxide surface by block copolymer lithography using self-assembled poly(styrene-*b*-ferrocenyldimethylsilane) films.[22] Silicates have been selectively mineralized in the acidified PEO microdomains of triblock and diblock copolymer films by introducing silicon alkoxides in supercritical carbon dioxide; calcination or plasma etching produced ordered mesoporous films.[12] Two research groups independently reported the use of perpendicularly oriented but disordered lamellar poly(styrene-*b*-4-vinylpyridine) for growth of nanoscale-patterned silica;[23−25] sol−gel chemistry selectively nucleated silicon oxide on the 4-vinylpyridine microdomains, and careful calcination produced networked silica films.[24] It has been demonstrated that mineralization can occur by reacting a copolymer film with tetraethoxysilane (TEOS) vapors.[25] Similarly, mesoporous films have been prepared by reaction of TEOS vapors with surfactant coatings.[26]

Block copolymer thin films with perpendicularly oriented cylindrical microdomains are particularly attractive templates for arrays of nanoscopic posts or dots. Interfacial interactions need to be controlled to prevent an orientation that is parallel to the substrate. Anchoring a random copolymer of styrene and methyl methacrylate (P(S-*r*-MMA)) with a styrene volume fraction of approximately 0.6 to a substrate can achieve the desired orientation for poly(styrene-*b*-methyl methacrylate) (P(S-*b*-MMA)) films.[27,28] Such films have been used to template silica nanoposts by selectively etching PMMA cylinders and filling the pores with silicon oxide by introduction of silicon tetrachloride under reduced pressure and with a trace amount of water.[29] This chemistry has also been used to create arrays of silicon oxide nanodots in poly(styrene-*b*-ethylene oxide) (P(S-*b*-EO)) thin films that have a perpendicular orientation of PEO cylinders.[30,31]

In this report, multiple strategies are explored for preparation of silica nanostructures from a molecular precursor using P(S-*b*-MMA) films with oriented cylindrical microdomains as templates. Nanometer-scale silica posts were synthesized by pore-filling and selective-mineralization routes through the use of TEOS in vapor-phase or liquid-phase reactions. Calcination removed the copolymer and resulted in arrays of standing silica nanostructures. The applicability of these nanostructured surfaces for the preparation of highly hydrophobic surfaces was investigated by functionalization of the surfaces with hydrophobic moieties. These techniques provide facile and reproducible processes for construction of lateral arrays of inorganic oxide nanostructures.

Experimental Section

Chemicals and Materials. P(S-*b*-MMA) with a molecular weight of 50 000 g mol^{-1}, a M_w/M_n ratio of 1.07, and a PS:PMMA volume fraction of 70:30 was synthesized by anionic polymerization. A random copolymer, P(S-*r*-MMA), with a terminal benzyl alcohol group and a molecular weight of 11 000 g mol^{-1}, a M_w/M_n ratio of 1.17, and a PS:PMMA volume fraction of 58:42 was used to balance the interfacial interactions of the PS and PMMA blocks with the substrate.[27] TEOS and denatured 85% ethanol (EtOH) (approximately 15% methanol) (Alfa Aesar), 5 N hydrochloric acid and glacial acetic acid (J. T. Baker), toluene (Aldrich), trimethylchlorosilane (TMS) (Gelest), and (tridecafluoro-1,1,2,2-tetrahydrooctyl)dimethylchlorosilane (FDCS) (Gelest) were used as received. Water was distilled and deionized to 18.3 MΩ cm. Silicon wafers (International Wafer Service) had thicknesses of 475−575 μm and native oxide layer thicknesses of approximately 20 Å.

Preparation of P(S-*b*-MMA) Thin Films on "Neutral Brush"-Coated Silicon. A silicon wafer was functionalized with the random copolymer P(S-*r*-MMA) by spin coating a thin film from a 1 wt % solution in toluene. This film was annealed under vacuum at 170 °C for 72 h to anchor the hydroxyl chain ends to the substrate, and then was rinsed with toluene to remove excess copolymer not anchored to the substrate to yield an anchored P(S-*r*-MMA) film of approximately 6-nm thickness; thinner P(S-*r*-MMA) films ultimately led to substandard P(S-*b*-MMA) films. P(S-*b*-MMA) was spin coated onto the modified substrate from a 1 wt % solution in

(17) Templin, M.; Franck, A.; DuChesne, A.; Leist, H.; Zhang, Y.; Ulrich, R.; Schädler, V.; Wiesner, U. *Science* **1997**, *278*, 1795.
(18) Simon, P. F. W.; Ulrich, R.; Spiess, H. W.; Wiesner, U. *Chem. Mater.* **2001**, *13*, 3464.
(19) Mahajan, S.; Renker, S.; Simon, P. F. W.; Gutmann, J. S.; Jain, A.; Zhang, Y.; Gruner, S. M.; Fetters, L. J.; Coates, G. W.; Wiesner, U. *Polym. Mater. Sci. Eng.* **2003**, *88*, 148.
(20) Renker, S.; Mahajan, S.; Babski, D. T.; Schnell, I.; Jain, A.; Gutmann, J.; Zhang, Y.; Gruner, S. M.; Spiess, H. W.; Wiesner, U. *Macromol. Chem. Phys.* **2004**, *205*, 1021.
(21) Chan, V. Z.-H.; Hoffman, J.; Lee, V. Y.; Latrou, H.; Avgeropoulos, A.; Hadjichristidis, N.; Miller, R. D.; Thomas, E. L. *Science* **1999**, *286*, 1716.
(22) Cheng, J. Y.; Ross, C. A.; Thomas, E. L.; Smith, H. I.; Vancso, G. J. *Appl. Phys. Lett.* **2002**, *81*, 3657.
(23) Cho, G.; Jang, J.; Jung, S.; Moon, I.-S.; Lee, J.-S.; Cho, Y.-S.; Fung, B. M.; Yuan, W.-L.; O'Rear, E. A. *Langmuir* **2002**, *18*, 3430.
(24) Fujita, N.; Otsuka, H.; Takahara, A.; Shinkai, S. *Chem. Lett.* **2003**, *32*, 352.
(25) Fujita, N.; Asai, M.; Yamashita, T.; Shinkai, S. *J. Mater. Chem.* **2004**, *14*, 2106.
(26) Nishiyama, N.; Tanaka, S.; Egashira, Y.; Oku, Y.; Ueyama, K. *Chem. Mater.* **2003**, *15*, 1006.
(27) Mansky, P.; Liu, Y.; Huang, E.; Russell, T. P.; Hawker, C. *Science* **1997**, *275*, 1458.
(28) Huang, E.; Rockford, L.; Russell, T. P.; Hawker, C. J. *Nature* **1998**, *395*, 757.
(29) Kim, H.-C.; Jia, X.; Stafford, C. M.; Kim, D. H.; McCarthy, T. J.; Tuominen, M.; Hawker, C. J.; Russell, T. P. *Adv. Mater.* **2001**, *13*, 795.
(30) Kim, D. H.; Jia, X.; Lin, Z.; Guarini, K. W.; Russell, T. P. *Adv. Mater.* **2004**, *16*, 702.
(31) Kim, D. H.; Kim, S. H.; Lavery, K.; Russell, T. P. *Nano Lett.* **2004**, *4*, 1841.

toluene and was annealed under vacuum at 170 °C for at least 15 h. The block copolymer film thickness measured by ellipsometry was typically 30−33 nm. Sample sizes were typically 1.5 cm × 1.5 cm or larger.

Preparation of P(S-*b*-MMA) Thin Films on Passivated Silicon. Silicon wafers were immersed in 5 wt % aqueous hydrofluoric acid for 5 min to remove the native oxide layer, then were rinsed with water and dried at 100 °C under vacuum for 1 h. P(S-*b*-MMA) was spin coated onto the passivated wafers and was annealed as described above.

Preparation of Porous PS Thin Films. P(S-*b*-MMA) films were exposed to UV radiation for 30 min under vacuum to degrade the PMMA blocks and to crosslink the PS matrix. Degraded PMMA was then removed by immersion in glacial acetic acid for 5 min, followed by rinsing in water.

Vapor-Phase Growth of Silicon Oxide in Porous PS Thin Films and in P(S-*b*-MMA). Films were dried under vacuum at 65 °C overnight immediately prior to use in mineralization experiments. A sample was placed at the center of the bottom of a 240-mL Teflon jar. Two open 6-mL vials, one of which contained 1 mL of neat TEOS and the other which contained 0.5 mL of 5 N aqueous hydrochloric acid, were placed inside the jar, diametrically against the container walls. The sealed jar was heated in an oven at 75 °C for 3−4 h.

Liquid-Phase Sol−Gel Growth of Silicon Oxide in Porous PS Thin Films and in P(S-*b*-MMA). A sol of typical molar composition 1 TEOS:4 H_2O:4 EtOH:0.12 acetic acid was used for mineralization of P(S-*b*-MMA) films. Samples were immersed in the sol for 10−72 h at RT (approximately 22 °C), rinsed with water, and dried under vacuum at 65 °C for 6 h.

Calcination. Samples were placed in alumina crucibles and calcined in a muffle furnace. The temperature was ramped at 1 °C min^{-1} to 400 °C under flowing N_2, then raised 1 °C min^{-1} to 500 °C under flowing air (79 mol % N_2, 21 mol % O_2), and heated at 500 °C for 5 h.

Reaction of Substrates with Organosilanes. A procedure reported by Fadeev et al.[6] was adapted to functionalize selected samples with alkyl and fluorinated alkyl groups. Samples were immersed in piranha solution (70 vol % H_2SO_4, 30 vol % of 30 wt % H_2O_2) (caution: piranha solution is highly corrosive and can be explosive) overnight at RT, rinsed with copious amounts of H_2O, and dried at 120 °C for 2 h. Each sample was then placed in a closed 240-mL Teflon jar that also contained 0.5 mL of a chlorosilane reagent in an open 6-mL vial; the films did not come in direct contact with liquid chlorosilane reagents. The sealed jars were heated in an oven for 4 d at 60 °C (TMS) or at 70 °C (FDCS). TMS was replenished periodically because of its high vapor pressure and concern that too much might escape the reaction jar. Replenishment was not necessary for FDCS, and liquid remained after 4 d. The functionalized samples were rinsed with toluene (2 aliquots), ethanol (3 aliquots), 1:1 ethanol:water (2 aliquots), water (2 aliquots), ethanol (2 aliquots), and water (3 aliquots) and then dried at 120 °C for 30 min.

Characterization. Scanning force microscopy (SFM) measurements were performed using a Dimension 3000 system from Digital Instruments, Inc. Images were acquired in tapping mode under ambient conditions using silicon cantilevers with a resonant frequency of 300 kHz and a spring constant of 42 N m^{-1}. Images were "flattened" using Nanoscope IIIa software. X-ray photoelectron spectroscopy (XPS) was performed on a Perkin-Elmer Physical Electronics 5100 with Mg Kα excitation (15 kV, 400 W). Angle-resolved measurements were made by setting the detector at 15° and 75° takeoff angles with respect to the surface plane. A Rudolph Research AutoEL II automatic ellipsometer with a helium−neon laser (λ = 632.8 nm) was used to measure film thickness at an incident angle of 70° from the surface normal. Contact angle measurements were performed using a Ramé-Hart telescopic goniometer equipped with a Gilmont syringe having a 24-gauge flat-tipped needle. Purified water was used as the probe fluid; advancing (θ_A) and receding (θ_R) contact angles were determined as the volume of the probe fluid was being increased and decreased, respectively. The values reported are the averages of at least three measurements.

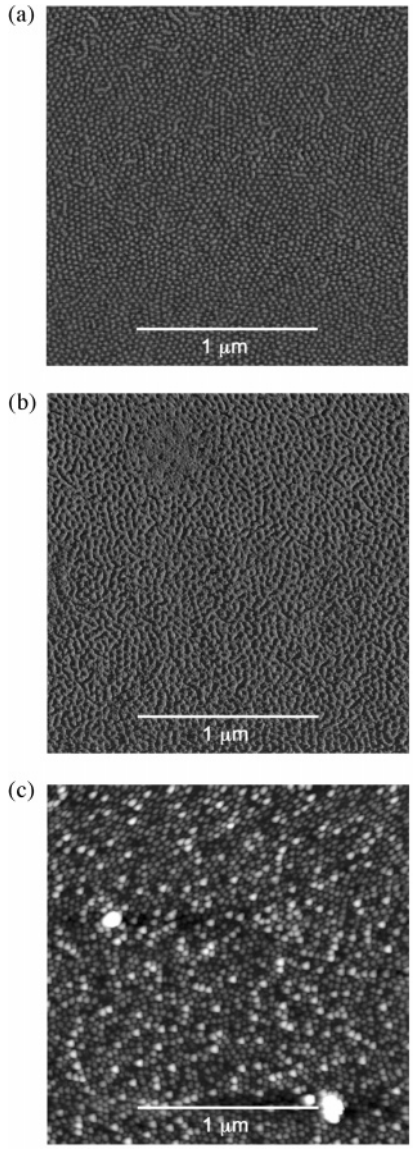

Figure 1. (a) SFM phase contrast image of P(S-*b*-MMA) spin coated on passivated silicon and annealed at 170 °C (*z* range = 30°); (b) SFM phase contrast image of the corresponding porous PS film (*z* range = 60°); (c) SFM height contrast image of silica nanostructures prepared by exposure of the porous PS film to TEOS and HCl vapors at 75 °C for 3.5 h and calcination at 500 °C (*z* range = 30 nm).

Results and Discussion

Silicon Oxide Growth in Porous PS Thin Films. SFM images of P(S-*b*-MMA) films spin coated on passivated silicon showed grains of hexagonally packed PMMA cylindrical microdomains oriented normal to the film surface (Figure 1a). The average center-to-center distance between PMMA cylinders was 32 nm. Etching of the PMMA

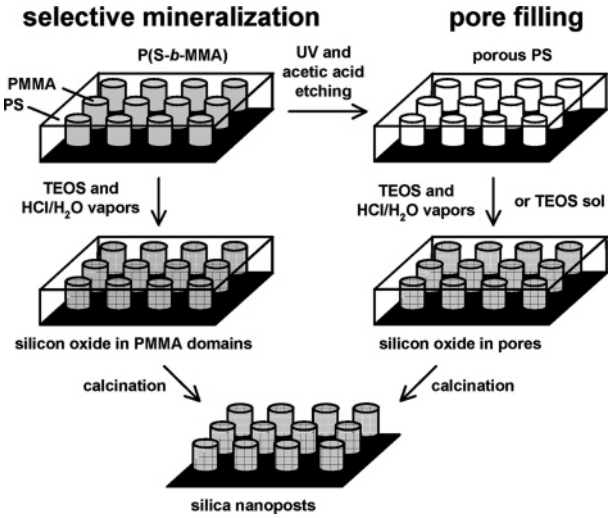

Figure 2. Two routes for preparation of silica nanostructures in P(S-*b*-MMA) thin films: selective mineralization, in which silicon oxide is deposited in PMMA cylinders, and pore filling, in which silica replaces porous volume after etching the PMMA microdomains.

microdomains using UV light and acetic acid yielded thin films with pores that were continuous to the silicon substrate[29] (Figure 1b).

A pore-filling route to fabricating silica nanostructures using sol−gel chemistry was investigated (Figure 2). Exposure of a porous template to TEOS and 5 N HCl vapors at 75 °C for 3.5 h did not lead to complete pore filling, but some extraneous silica deposits were observed on the surface of the PS. Nanostructures that were relatively uniform in height and diameter were observed after calcination in air (Figure 1c). A 4-h vapor-phase experiment overfilled the pores and formed silica "mushrooms" that reproduced the short-range hexagonal order of the template. There was little change in appearance of the nanostructures after calcination of the PS. Colored growth fronts were visible by eye at the edges of the films, which is indicative of uncontrolled silica growth, as discussed below.

Immersion of a porous PS film in a TEOS sol at RT for 24 h did not alter its appearance by SFM; the pores were open and no extraneous deposits were apparent on the surface, in contrast to vapor-phase experiments. Angle-resolved XPS experiments detected silicon oxide at both 15° and 75° takeoff angles. However, elemental silicon due to the substrate (Si_{2p} peak at 100 eV) was detected only with the 75° takeoff angle. This differed from a porous unreacted PS film where silica was barely detectable. The sample that was immersed in the TEOS sol was soaked again for 18 h at RT. Although the pores were not completely filled, uniform silica nanoposts were evident by SFM images of the sample after calcination.

SFM images of P(S-*b*-MMA) on neutral brush-modified silicon exhibited distinct grains of hexagonally packed cylindrical microdomains oriented normal to the surface (Figure 3a). Exposure to UV light, followed by rinsing in acetic acid, removed the PMMA, resulting in cylindrical pores.

Treatment of a porous template for 3 h at 75 °C with TEOS and 5 N HCl vapors did not completely fill the pores, but the colored edges of the film indicated that some silica

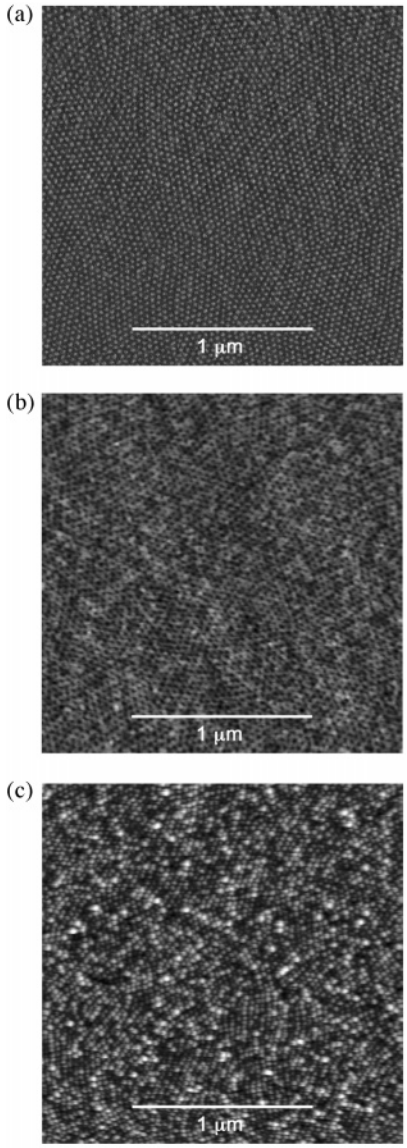

Figure 3. (a) SFM phase contrast image of P(S-*b*-MMA) spin coated on neutral brush-modified silicon and annealed at 170 °C (*z* range = 30°); (b) SFM height contrast image of the corresponding porous PS film immersed in a TEOS sol at RT for 72 h (*z* range = 10 nm); (c) SFM height contrast image of the silica nanostructures after calcination at 500 °C (*z* range = 15 nm).

growth had occurred. Calcination at 500 °C resulted in an array of silica nanoposts approximately 5 nm in height.

Immersion of the porous template in a TEOS sol at RT for 72 h did not lead to complete pore filling, but uniform silica posts approximately 10 nm in height were apparent upon removal of the PS template (Figure 3b, c). Grains of hexagonal order were evident, and little extraneous silica growth occurred on the surface. Colored growth fronts were not observed at the edges of the sample.

Vapor-Phase Silicon Oxide Mineralization in P(S-*b*-MMA) Thin Films. Experiments were performed to grow silicon oxide in the PMMA microdomains, as illustrated in Figure 2. Mineralization of a P(S-*b*-MMA) film on neutral brush-modified silicon was noticeable after exposure to TEOS and 5 N HCl vapors at 75 °C for 3 h. SFM height contrast images showed that the PMMA microdomains protrude slightly above the surface, with an increase from approximately 2 nm in the original template to approximately

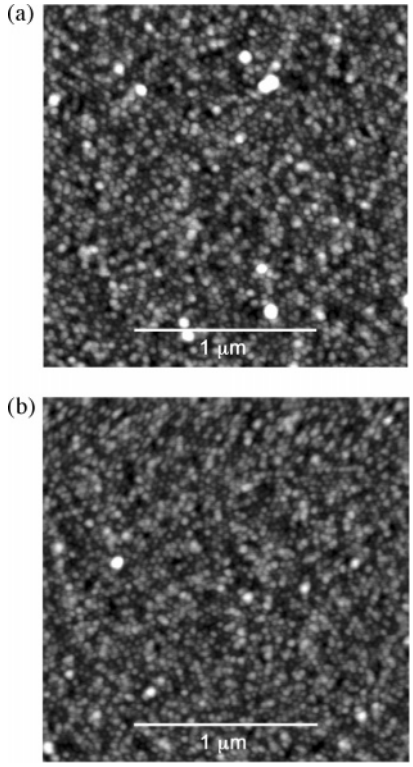

Figure 4. (a) SFM height contrast image of a mineralized P(S-*b*-MMA) film prepared by exposure to TEOS and HCl vapors at 75 °C for 4 h (*z* range = 20 nm); (b) SFM height contrast image after calcination at 500 °C (*z* range = 15 nm).

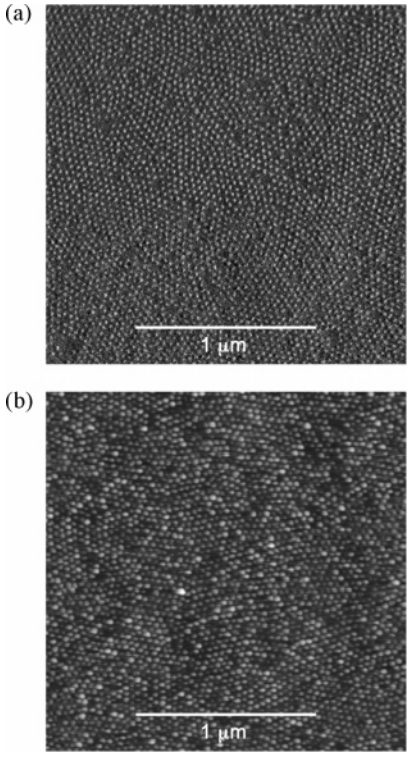

Figure 5. (a) SFM phase contrast image of a substandard P(S-*b*-MMA) film with some missing PMMA microdomains (*z* range = 20°); (b) SFM height contrast image after exposure to TEOS and HCl vapors at 75 °C (*z* range = 20 nm).

5 nm. Some larger extraneous growths were also seen. The existence of silicon oxide was confirmed by XPS; the Si_{2p} peak was observed at 102 eV and the intensity of the O_{1s} peak was much greater than that observed for the original copolymer. However, calcination of the film at 500 °C did not result in any regular silicon oxide structures. Silicon oxide mineralization was more extensive after a 4-h reaction. The mineralized PMMA microdomains appeared to impinge on each other at the surface, yet they still displayed the hexagonal order of the template (Figure 4a). SFM images of the sample were nearly identical after calcination, indicating the existence of standing silica nanostructures (Figure 4b). However, the height of the silica nanoposts appeared to be significantly shorter than the 30-nm thickness of the film template.

Contraction of silica nanoposts would be expected during calcination as the extent of silicon oxide condensation increases. Cracks that were observable under an optical microscope appeared throughout the surface, resulting in platelike sections that were tens to hundreds of micrometers in size. The depth of the cracks allowed the thickness of nanostructured silica to be estimated at approximately 16 nm by SFM. Cracking was a common feature in samples where silicon oxide growth was evident on the surface of the template. The occurrence of cracking suggests that silicon oxide mineralization of the copolymer did not extend to the native oxide layer of the wafer. Upon calcination, degradation of the PMMA allowed the silicon oxide in the cylinders to bond to the substrate. The difference in the coefficients of thermal expansion of silicon oxide and the copolymer led to cracking of silicon oxide when the temperature exceeded the glass transition temperature (T_g) of the copolymer.

The high selectivity of silicon oxide growth for the PMMA domains was demonstrated using substandard templates. P(S-*b*-MMA) templates were prepared such that there were areas of the surface where the PMMA microdomains were absent (Figure 5a). Exposure to TEOS and HCl vapors resulted in regular growths on the surface of the film with occasional bare patches that resembled the original template (Figure 5b).

Vapor-phase mineralization is advantageous because of the ease with which silica nanoposts can be templated using benchtop methods. However, the occurrence of irregular silica growths can be problematic, and it was difficult to generate surfaces with growths that were consistently as discrete and regular as those in Figure 3b. In addition, the appearance of colored growth fronts from the edges of the film indicated areas where the silicon oxide formation was uncontrolled, which may be due to penetration of the TEOS, HCl, and water vapors into the neutral brush layer from the side as well as from the surface of the film.

Silicon Oxide Mineralization in Reconstructed P(S-*b*-MMA) Thin Films. Reconstruction of a P(S-*b*-MMA) thin film in the presence of a selective solvent has been reported.[32,33] Acetic acid, which is a good solvent for PMMA, swells the cylindrical microdomains. The PMMA chains, which are covalently linked to insoluble PS chains, are drawn to the surface and cover the PS matrix. This change produces a nanoporous film that has pores smaller in diameter than those obtained by fully removing the PMMA, with no change

(32) Xu, T.; Stevens, J.; Villa, J.; Goldbach, J. T.; Guarini, K. W.; Black, C. T.; Hawker, C. J.; Russell, T. P. *Adv. Funct. Mater.* **2003**, *13*, 698.
(33) Xu, T.; Goldbach, J. T.; Misner, M. J.; Kim, S.; Gibaud, A.; Gang, O.; Ocko, B.; Guarini, K. W.; Black, C. T.; Hawker, C. J.; Russell, T. P. *Macromolecules* **2004**, *37*, 2972.

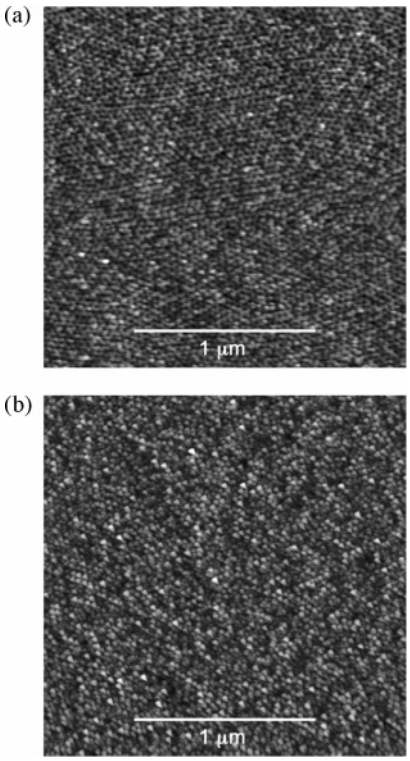

Figure 6. (a) SFM height contrast image of a P(S-*b*-MMA) film on neutral brush-modified silicon after immersion in a TEOS sol at RT for 10 h (z range = 12 nm); (b) SFM height contrast image after calcination at 500 °C (z range = 10 nm).

in the lattice spacing. The solvent reconstruction is reversible; annealing the thin film above its T_g regenerates the original copolymer film.

Immersion of a P(S-*b*-MMA) thin film template in an acetic acid containing TEOS sol led to restructuring of the film as described above (Figure 6a). Sols that used HCl in lieu of acetic acid also swelled the PMMA blocks and induced the formation of nanopores; the combination of organic solvent and acidic pH was effective at reconstructing the film. Angle-resolved XPS detected silicon oxide on a template treated with a TEOS sol for 10 h at RT; 1.0% Si was detected at a 15° takeoff angle, and 0.8% Si was detected at 75° (elemental analysis by XPS is not quantitatively accurate, but it is used here for comparison). These observations suggest that silicon oxide is deposited both in the pores and in the PMMA microdomains of the reconstructed film (Figure 7). Immersion of a template in the TEOS sol for 47 h yielded a relatively larger amount of silicon oxide detected by XPS (17.6% Si at 15°, 11.4% Si at 75°). However, the surface appeared to be much rougher when imaged by SFM, with the nanopores barely observable in a height contrast image.

Calcination of these samples at 500 °C resulted in silica nanoposts of a uniformity similar to those grown in porous PS thin films (Figure 6b). Although silicon oxide appeared to also be present within the PMMA microdomains of the reconstructed film prior to calcination, it did not contribute significantly to the silica nanostructures that remained after calcination. Reconstructed P(S-*b*-MMA) thin films were also prepared by preswelling in acetic acid, rinsing, and drying. Mineralization of these films by the vapor-phase method for 3−3.5 h led to similar nanostructures that were observable

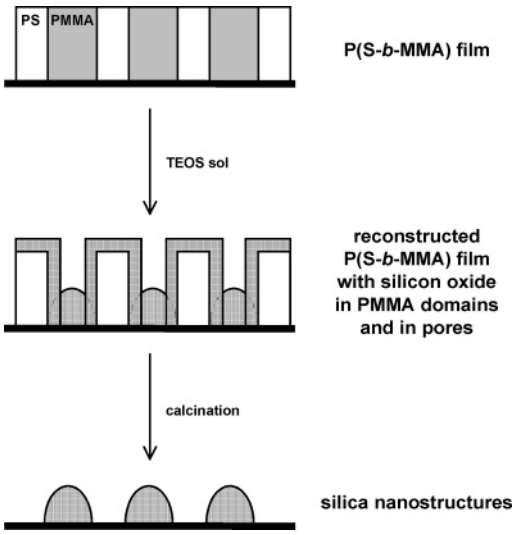

Figure 7. Reconstruction and mineralization of a P(S-*b*-MMA) thin film in a TEOS sol, with subsequent calcination to produce silica nanostructures.

by SFM after calcination. Longer reaction times produced obvious silica deposits on the surface, with no nanometer-scale order.

Dynamic Water Contact Angle Measurements on Alkyl- and Fluoroalkyl-Functionalized Silicon Oxide Nanostructures. The utility of these nanostructured silicon oxide surfaces for preparation of ultrahydrophobic surfaces was investigated. Wenzel has argued that the hydrophobicity of a material is enhanced by surface topography,[34] and a texture that allows air to be trapped under a drop is expected to do this most effectively.[35,36] The topographical details of a rough surface, such as the shape and arrangement of surface structures, have a significant influence on contact angle hysteresis.[7,37]

Nanoposts prepared by immersion of a P(S-*b*-MMA) template in a TEOS sol for 24 h at RT and calcination at 500 °C were functionalized by vapor-phase reaction with trimethylchlorosilane (TMS) or (tridecafluoro-1,1,2,2-tetrahydrooctyl)dimethylchlorosilane (FDCS). For comparison, the native oxide surfaces of silicon wafers (Si) were also modified with these organosilanes. Dynamic contact angle measurements were taken while increasing and decreasing the volume of a water droplet. TMS-functionalized nanoposts had advancing (θ_A) and receding (θ_R) contact angles of 141° and 87°, respectively, whereas FDCS-functionalized nanoposts yielded a θ_A/θ_R of 147°/ 101°. Values for θ_A/θ_R were 98°/91° and 110°/99° for TMS−Si and FDCS−Si, respectively.

There is notable hysteresis in the contact angles measured for the nanostructured surfaces, which indicates pinning of the water droplets. Significant hysteresis has also been observed with FDCS-functionalized silica nanoposts in a previous report.[29] Possible origins for the hysteresis in the contact angles are surface roughness and chemical heterogeneities because of incomplete coverage. Silylation of the

(34) Wenzel, W. R. *Ind. Eng. Chem.* **1936**, *28*, 988.
(35) Quéré, D. *Physica A* **2002**, *313*, 32.
(36) Bico, J.; Thiele, U.; Quéré, D. *Colloids Surf., A* **2002**, *206*, 41.
(37) Chen, W.; Fadeev, A. Y.; Hsieh, M. C.; Öner, D.; Youngblood, J.; McCarthy, T. J. *Langmuir* **1999**, *15*, 3395.

surfaces was expected to be as complete as possible on the basis of the literature report,[6] although it was not verified quantitatively in this work. The rather large values measured for θ_A on the nanostructured surfaces described here indicate that a much higher density of functional groups can be obtained relative to a flat surface.

Conclusion

P(S-*b*-MMA) thin films with cylindrical microdomains oriented normal to the surface have been used as templates for lateral arrays of nanoscopic silica structures. Silicon oxide has been introduced by simple vapor-phase or liquid-phase sol−gel reactions using TEOS, following either a pore-filling or a selective-mineralization route. Vapor-phase reactions more rapidly deposited silicon oxide in P(S-*b*-MMA) and porous PS thin films, whereas liquid sols very effectively produced nanostructures with a high degree of uniformity. Use of a TEOS sol led to a reconstruction of P(S-*b*-MMA) templates to form nanopores that were mineralized with silicon oxide. Silica nanostructures with the short-range hexagonal order of the templates were present after careful calcination of samples prepared by all processes. Functionalization of nanoposts with hydrophobic organosilanes resulted in high advancing water contact angles (>140°) because of nanometer-scale roughness, which demonstrates that a nanostructured surface can provide a higher density of functional groups than a flat surface for potential applications. The thin films used as templates in this report typically had a thickness in the range 30−33 nm, which is approximately the lattice spacing of the microphase-separated copolymer. It should be possible to obtain higher aspect ratio silica nanoposts through the use of thicker P(S-*b*-MMA) templates oriented with the aid of a reinforcing homopolymer[38] or an electric field.[39] The size of the silica nanostructures should also be influenced by choice of copolymer molecular weight or by addition of a miscible homopolymer to expand the microdomains.[40]

The benchtop sol−gel experiments described here can be applied to other block copolymers. In particular, standing silica nanostructures have been templated using P(S-*b*-EO) thin films with oriented cylindrical microdomains. Current work with P(S-*b*-MMA) in our laboratory has also produced ordered arrays of titanium oxide nanostructures, which should increase the range of potential applications for these templated inorganic oxide surfaces.

Acknowledgment. This work was supported by the Army Research Laboratory Polymer Materials Center of Excellence at the University of Massachusetts Amherst, the NSF-supported Materials Research Science and Engineering Center on Polymers at the University of Massachusetts Amherst, and the Department of Energy Office of Basic Energy Sciences.

CM051407B

(38) Jeong, U.; Ryu, D. Y.; Kho, D. H.; Kim, J. K.; Goldbach, J. T.; Kim, D. H.; Russell, T. P. *Adv. Mater.* **2004**, *16*, 533.
(39) Thurn-Albrecht, T.; DeRouchey, J.; Russell, T. P.; Jaeger, H. M. *Macromolecules* **2000**, *33*, 3250.
(40) Jeong, U.; Kim, H.-C.; Rodriguez, R. L.; Tsai, I. Y.; Stafford, C. M.; Kim, J. K.; Hawker, C. J.; Russell, T. P. *Adv. Mater.* **2002**, *14*, 274.